Journal of the Meteorological Society of Japan, Vol. 73, No. 2B, pp. 639–643, 1995

NOTES AND CORRESPONDENCE

Sea Surface Measurement by a Self-Contained Upward-Looking ADCP

By Hideo Nakajima, Arata Kaneko, Noriaki Gohda

Faculty of Engineering, Hiroshima University Higashi-Hiroshima 724, Japan

and

Kazuo Kawatate

Research Institute for Applied Mechanics, Kyushu University Kasuga 816, Japan

(Manuscript received 8 September 1994, in revised form 15 February 1995)

Abstract

Self-contained upward-looking ADCP data obtained at station (2°0.21′N, 156°0.11′E) during the TOGA/COARE IOP were carefully analyzed to extract the echo amplitude (AGC) returning from the sea surface. The AGC values at the surface were found to have a good correlation with the wind speed data obtained from the ATLAS buoy at the same site and ranging from 0 to 13 ms^{-1}. This study opened the possibility of predicting the wind speed from the surface AGC although the reason why backscatter from the sea surface increased with the wind speed was not sufficiently elucidated.

1. Introduction

The near-surface layer is one of the most difficult targets in the upward-looking ADCP (Acoustic Doppler Current Profiler) measurement because the near-surface data obtained by using the main lobe beam are severely contaminated by surface returns of the side lobe beams (Schott, 1986; Schott and Johns, 1987). Bubbles entrained from the atmosphere into the ocean are known to dominate backscatter from the near-surface layer when winds become strong (Thorpe, 1986; Crawford and Farmer, 1987). The fine structures on the wind-wave surface may also be used as scatterers, not only for the microwave observation from the satellite but also for the upward-looking ADCP observation. No attempt was made, however, to measure backscatter from the sea surface by an upward-looking ADCP.

In this paper, we attempt to extract the sea surface data from the profiling data obtained in the western equatorial Pacific by a self-contained upward-looking ADCP. The surface AGC (an indicator of echo amplitude) and velocities are compared with the wind speed obtained at the same site by an ATLAS (Autonomous Temperature Line Acquisition System) buoy.

2. Site and method

The moored ADCP observation was carried out at St.2N (2°0.21′N, 156°0.11′E) and St.2S (1°57.74′S, 156°0.44′E) during the TOGA/COARE IOP (Tropical Ocean Global Atmosphere/Coupled Ocean-Atmosphere Response Experiment Intensive Observing Period). Only the data obtained at St.2N during 5–14 Nov 1992 when a westerly burst blew are used for detailed analysis in this paper. The ADCP at St.2N was mounted upward in the float at the top of the mooring line (Kaneko *et al.*, 1993). The depth of the ADCP below the surface, measured by a pressure sensor, was 172 m. The 153 kHz ADCP with four transducers in the JANUS arrangement emitted sound beams at an angle of 20° from the vertical. The bin length and sampling time were set to 8.7 m and 15 min, respectively. The bin length was changed to 9 m after a correction using the temperature at the ADCP depth (Schott and Johns, 1987). A dual tilt sensor stored inside the ADCP measured the slant of the mooring line.

Figure 1 is the illustration showing the basic concept of the surface measurement by an upward-looking ADCP. The ADCP measures the echo am-

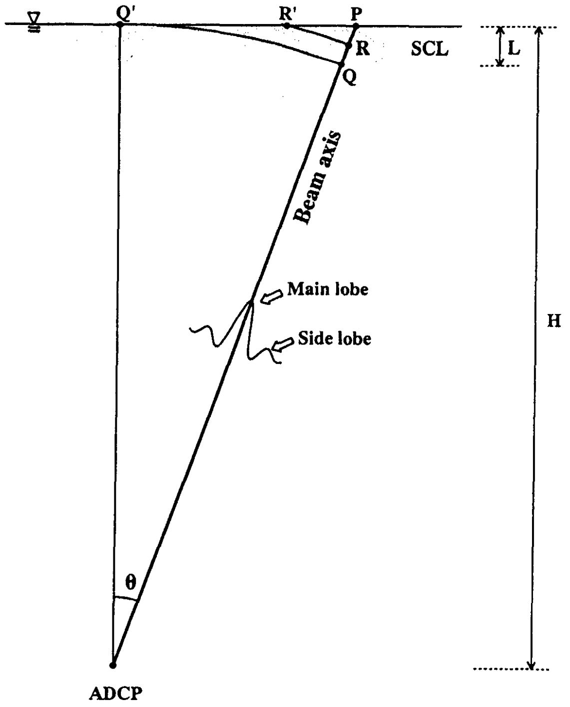

Fig. 1. Illustration showing the basic concept of the measurement of surface velocity by an upward-looking ADCP.

plitude itself and the current velocities by receiving the Doppler-shifted echoes reflected from sound scatterers in the water. The echo amplitude is recorded as AGC (automatic gain control) in this ADCP system. When the main lobe beam emitted reaches the point Q (R), the main lobe echoes are contaminated by surface returns of the side lobe beam from the point Q′ (R′). Thus in the upward-looking ADCP measurement, a side-lobe contaminated layer (SCL) forms near the surface (Kaneko and Ito, 1994). The thickness L of SCL is expressed by

$$L = H(1 - \cos\theta), \tag{1}$$

where H is the distance from the transducer to the surface and θ the angle of the beam axis from the vertical. Putting $H = 172$ m and $\theta = 20°$, we estimate L as 10 m. We can also see that the surface returns of the main lobe beam at point P have no contamination due to the side lobe beam and give us correct surface AGCs and velocities.

Wind data at 4 m height above the sea surface are supplied from the ATLAS buoy at (2°0.0′N, 156°0.0′E) which is part of the TOGA/TAO (Tropical Atmosphere Ocean) array deployed over the whole basin of the equatorial Pacific (McPhaden, 1993).

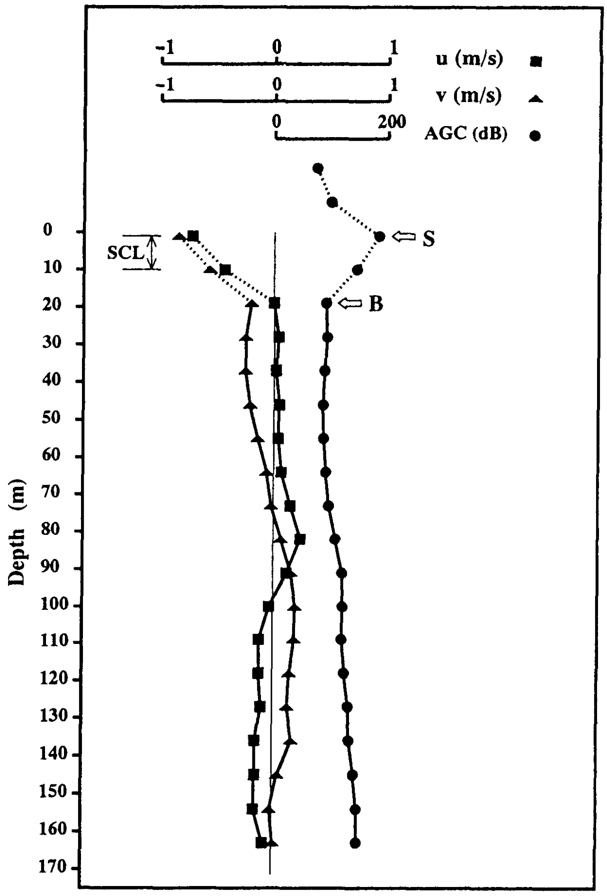

Fig. 2. A typical example of the vertical profiles of horizontal velocities and AGC: u, v denote the east and north components of velocity, respectively. The side-lobe-contaminated layer is indicated by the dotted lines.

3. Results

Figure 2 shows typical vertical profiles of AGC and horizontal velocities. The point S taken on the depth bin making a near-surface peak of AGC was in good agreement with the position of sea surface determined from the pressure sensor. The AGC data in the upper 10 m were contaminated by surface returns of the side lobe echoes and biased toward high values. The point B is put on the depth bin which is closest to the bottom of the SCL. Hereinafter, we call the AGC and velocities at the point S the surface AGC (SAGC) and surface velocity (SV), respectively, and call the velocities at the point B the near-surface velocity (NSV). In contrast with SV, NSV can not respond instantly to local winds. The tidal current and the ocean current generated by a basin-wide wind such as the Trades are likely to be constant over the near-surface layer. When the above two assumptions are justified, surface velocities generated by local winds may be determined

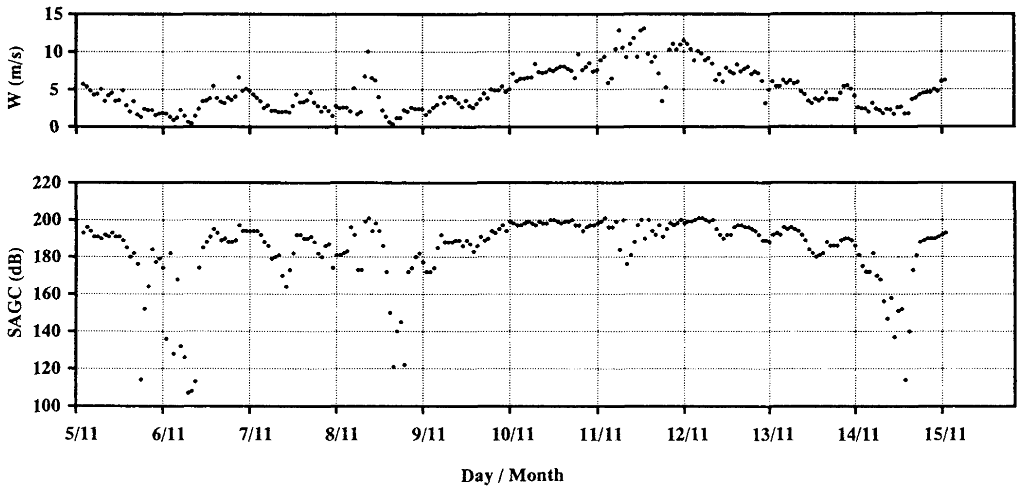

Fig. 3. Time plots of the SAGC and W.

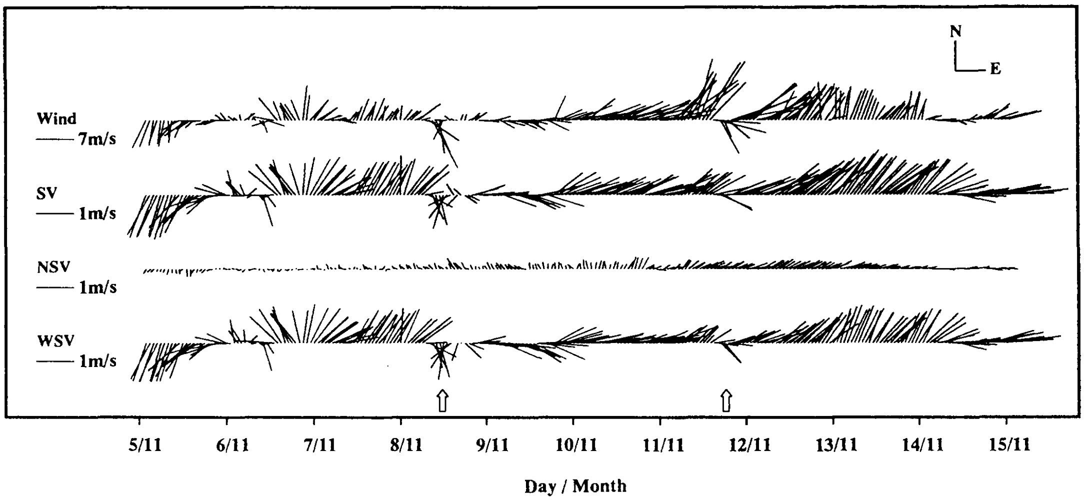

Fig. 4. Vector plots of SV, NSV, WSV and W. The times when the rapid changes of wind direction occurred are indicated by the open arrows.

through a subtraction of the NSV from the SV. We call this velocity difference the WSV (wind-induced surface velocity).

The hourly time plot of SAGC is shown in Fig. 3 together with that of the ATLAS wind. Agreement between both data was good in terms of overall features. Figure 4 shows the hourly vector plot of the ATLAS wind, SV, NSV and WSV. A westerly burst greater than 7 ms^{-1} blew during 10–12 Nov. In other periods, winds were relatively weak and variable. Rapid changes of wind direction occurred on 8 and 11 Nov as indicated by the open arrows. The directions of the SV and the WSV had a good correlation with the wind direction. Especially, the short-term variations of wind at the times indicated with the open arrows were well traced with the SV and WSV data. In contrast, the NSV did not follow the short-term variations of the wind.

Figure 5 shows the values of SAGC plotted against the ATLAS wind speed (W). The SAGC rapidly increased with W for wind speeds less than 4 ms^{-1}. The increasing rate was appreciably reduced for W over 4 ms^{-1}. The correlation between SAGC and W was good over the whole range of wind speed. The correlation between the magnitude (V_s) of the WSV and W is shown in Fig. 6a. Roughly, V_s increased with increasing W until W reached about 5 ms^{-1} and decreased for larger W. The maximum value of V_s was about 1.3 ms^{-1} which was equated to one fourth of W. An empirical formula $V_s = 0.03W$ between the surface velocity and wind speed, used commonly, is drawn with a dotted line in this figure (Gill, 1982). For W ranging from 3 to 8 ms^{-1}, the values of V_s were much larger than those predicted by this formula. At smaller or larger W, the values of V_s were close to the dotted line. Figure 6b shows the correlation between the direction (θ_s) of the WSV and the direction (θ_w) of W. Almost

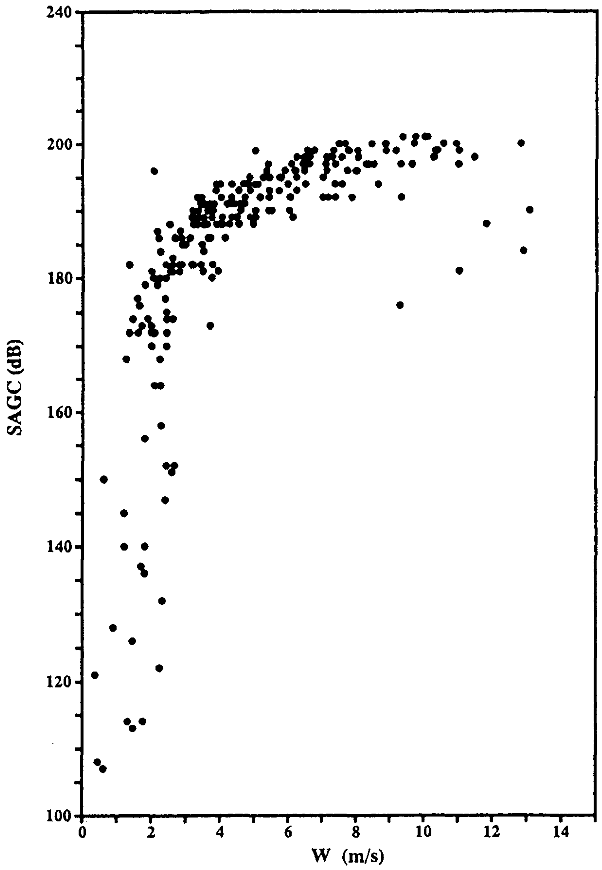

Fig. 5. Plot of SAGC against W.

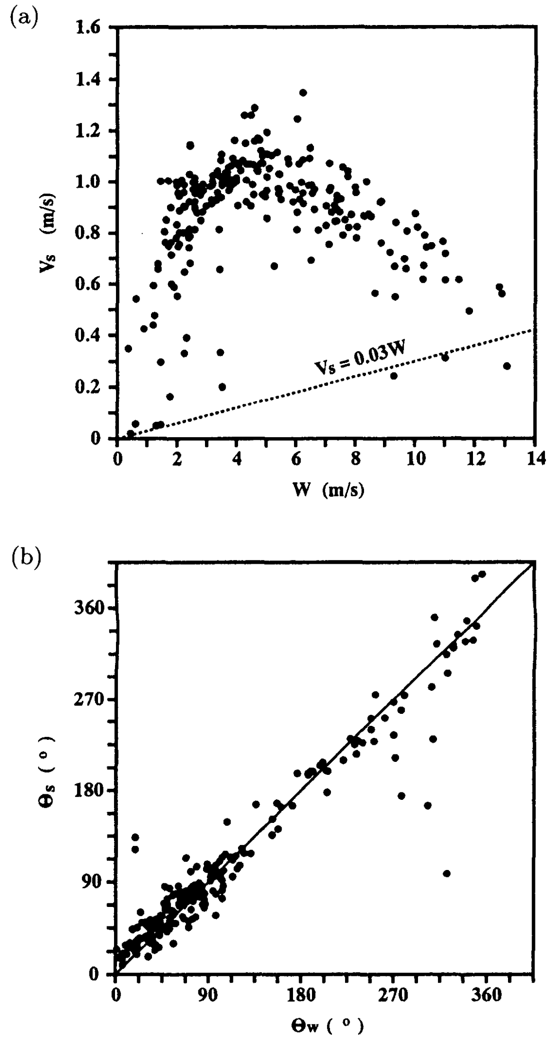

Fig. 6. Correlation between the wind and WSV. (a) Plot of V_s against W. (b) Plot of θ_s against θ_w.

all the data scattered near the solid line, indicating $\theta_s = \theta_w$.

4. Summary and discussion

We summarize the major results obtained in this study:

(1) The echo amplitude and velocities at the sea surface can be measured by the main lobe beam of the upward-looking ADCP without contamination due to the side-lobe beams.

(2) The AGC values at the surface increase with the wind speed W over the whole observation range. The increasing rate changes appreciably at 4 ms^{-1} of W.

(3) The magnitude (V_s) of the WSV increases with W up to 4 ms^{-1} and decreases drastically at larger W, approximating to the empirical formula $V_s = 0.03W$.

(4) The direction of WSV is in good agreement with that of the wind speed over the whole observation range.

From the above results we infer as follows. The result (2) suggests that the number of sound scatterers at and just below the sea surface increases with the wind speed. For wind speeds less than 4 ms^{-1}, scatterers may mainly be composed of wave-like fine structures on wind waves such as ripples (Valenzuela, 1978). For larger wind speeds, bubbles entrained into the near-surface layer from the atmosphere are likely to be responsible for the increase in the number of scatterers (Crawford and Farmer, 1987). The results (3) and (4) mean that contribution of the flow velocity on WSV is not significant in the moderate range of W. At large W, it seems that the increased number of bubbles serves for the ADCP to measure the flow velocity rather than the phase speed of wind waves.

It should be noted that sea-surface dynamics such as the growth of wind waves, the wave breaking and the generation of wind-driven current are controlled by many factors: wind speed, wind direction, fetch, *etc.* (Toba, 1988; Gill, 1982). This is our first report on the sea surface data obtained by the upward-looking ADCP. A more precise approach is required to understand sea surface processes from the upward-looking ADCP data.

Acknowledgments

We greatly appreciate Prof. A. Sumi of University of Tokyo and Prof. K. Takeuchi of Hokkaido University for their crucial contributions to the sophisticated planning and successful finish of the moored ADCP measurement in the J-COARE Program. Dr. T. Ito of Hiroshima University, Messrs. T. Nagahama, T. Shinozaki, A. Tashiro and T. Abe of Kyushu University and Mr. H. Furukawa of Kure Womans College are acknowledged for their essential rôles in the deployment and recovery of the moored ADCP system. We thank Dr. Michael J. Mcphaden, Director of the TOGA-TAO Project Office for the kind supply of the ATLAS wind data. We also thank the captains and crews of the R.V. Hakuho Maru of the University of Tokyo and the R.V. Natsushima of the Japan Marine Science and Technology Center for their assistance with shipboard work.

References

Crawford, C.B. and D.M. Farmer, 1987: On the spatial distribution of ocean bubbles. *J. Geophys. Res.*, **92**, 8231–8243.

Gill, A.E., 1982: *Atmosphere-Ocean Dynamics.* Academic Press, New York, 662 pp.

Kaneko, A., N. Gohda, H. Nakajima, T. Itoh, K. Kawatate, T. Nagahama and H. Hurukawa, 1993: Profiling measurement of the equatorial currents by an ADCP on the mooring lines. *In Preliminary Report of the Hakuho Maru Cruise KH-92-5*, T. Asai, Ed., Ocean Research Institute, University of Tokyo, 36–55.

Kaneko, A. and T. Ito,1994: Prevalence of ADCP and the associated progress of oceanography. *Umi no Kenkyu*, **3**, 359–372 (in Japanese).

McPhaden, M.J., 1993: TOGA-TAO and the 1991–93 El Nino-Southern Oscillation event. *Oceanography*, **6**, 36–43.

Schott, F., 1986: Medium-range vertical acoustic Doppler current profiling from submerged bouys. *Deep-Sea Res.*, **33**, 1279–1292.

Schott, F. and W. Johns ,1987: Half-year-long measurements with a buoymounted acoustic Doppler current profiler in the Somali Current. *J. Geophys. Res.*, **92**, C5, 5169–5176.

Thorpe, S., 1986: Bubble clouds: a review of their detection by sonar, of related models, and of how Kv may be determined. *In Oceanic White-caps*, D. Reidel, Norwell, Mass., 57–68.

Toba, T., 1988: Similarity laws of the wind wave and the coupling process of the air and water turbulent boundary layers. *Fluid Dyn. Res.*, **2**, 263–279.

Valenzuela, G.R., 1978: Theories for the interaction of electromagnetic and oceanic waves — A review. *Boundary-Layer Meteolor.*, **13**, 61–85.

自己記録式上方設置型 ADCP による海面計測

中嶋秀夫・金子　新・江田憲彰

(広島大学工学部)

川建和雄

(九州大学応用力学研究所)

TOGA/COARE IOP 期間中に、測点 (2°0.21′N, 156°0.11′E) で得られた自己記録式上方設置型 ADCP データを注意深く解析し、海面からの散乱音波振幅 (AGC) を抽出した。海面における AGC 値は、同測点における ATLAS ブイによる 0 から 13 ms^{-1} まで変動した風速とよい相関を持つことが分かった。海面からの後方散乱が風速と共に増大する理由については十分に解明されなかったが、この研究により風速が海面での AGC 値から予測できる可能性が開かれた。